

## Manipulate dynamic chemical interactions in renewable polymers for 3D printing tunable, healable, and recyclable metamaterials

Yuchao Wu <sup>a</sup>, Cheng Qiu <sup>a</sup>, Karla J. Silva <sup>b</sup>, Jaeho Shin <sup>b</sup>, Shaoyun Wang <sup>a</sup>, Bujingda Zheng <sup>a</sup>, Zhenru Chen <sup>a</sup>, Guoliang Huang <sup>a</sup>, James M. Tour <sup>b,c,d</sup>, Jian Lin <sup>a,\*</sup>

<sup>a</sup> Department of Mechanical and Aerospace Engineering, University of Missouri, Columbia, MO 65211, United States

<sup>b</sup> Department of Chemistry, NanoCarbon Centre and the Rice Advanced Materials Institute, Rice University, 6100 Main Street, Houston, TX 77005, United States

<sup>c</sup> Department of Materials Science and NanoEngineering, NanoCarbon Centre and the Rice Advanced Materials Institute, Rice University, 6100 Main Street, Houston, TX 77005, United States

<sup>d</sup> Department of Computer Science Engineering, NanoCarbon Centre and the Rice Advanced Materials Institute, Rice University, 6100 Main Street, Houston, TX 77005, United States

### ARTICLE INFO

**Keywords:**

### ABSTRACT

Mechanical metamaterials have garnered significant interests due to their unique properties, which arise from the periodic structures of their constituent units. However, traditional mechanical metamaterials suffer from limitations of fixed properties of the constituent units or irreversibility if they are damaged or little-to-no recyclability. Addressing this challenge, herein, a photoresin consisting of a monomer synthesized from a renewable biomass—epoxidized soybean oil (ESO)—citric acid (CA) and other components was developed for light-based 3D printing. It is discovered that the UV irradiation initiates photopolymerized of the highly photoactive epoxidized soybean oil-ethyl acrylamide (ESO-EA) monomer while enabling the epoxy-acid reaction (EAR) of the epoxy groups in ESO-EA with carboxyl groups in CA to create dynamic chemical bonds (DCBs). This formed dynamic crosslinking network endows the printed material with tunable tensile strengths (0.3–10.4 MPa) and shape memory behaviors (transition temperature: 22–48 °C) while maintaining high stretchability (fracture strain: 81 %–205 %). Thermal annealing facilitates dynamic transesterification reactions (DTER) to further improve the mechanical properties while making the printed materials healable and recyclable. By integrating these innovations into liquid crystal display (LCD) based 3D printing, we demonstrate origami metamaterials with tunable, multi-stable mechanical behaviors as well as property recovery after self-healing of the damaged structures by both simulations and experiments. Finally, the printed metamaterials can be recycled with the well-preserved properties.

### 1. Introduction

Mechanical metamaterials are engineered materials with properties that are not found in natural materials [1,2]. They derive their unique characteristics from the periodic arrangement and geometry of their constituent units. Traditional mechanical metamaterials have fixed properties once their constituent units are fabricated. In contrast, tunable mechanical metamaterials take this concept a step further by incorporating active units that can dynamically respond to external stimuli, such as changes in temperature and mechanical loading or applied electric and electromagnetic fields [3,4]. Development of these active metamaterials is driven by the desire to create materials with

adaptive and tunable mechanical properties by dynamically controlling and adjusting the constituent units made from smart materials such as shape-memory alloys, piezoelectric materials, or magnetostrictive materials [5–7]. As a result, they exhibit diverse and fascinating behaviors, opening up new possibilities for mechanical wave manipulation which extend beyond the reach of traditional metamaterials [8,9]. Another challenge in the metamaterial field is that their properties are sensitive to the change of the constituent units, which is often irreversible if damaged. While these unique constituent units require dedicated fabrication techniques such as 3D printing [10,11], they lead to high cost of the mechanical metamaterials. Thus, from the economy and performance perspectives, fabrication of mechanical metamaterials—which

\* Corresponding author.

E-mail address: [linjian@missouri.edu](mailto:linjian@missouri.edu) (J. Lin).

are active and tunable, robust to the performance degradation due to the unit damage meanwhile being healable, and recyclable after end-of-life use—is highly desirable while remaining a grand challenge that is largely underexplored. This challenge mainly arises from the lack of a suitable material, which has the uniquely combinational properties of being tunable or responsive to external stimulations, healable, recyclable and printable. This gap forms a technical barrier to the next-generation metamaterial development.

To tackle the challenge, the first obstacle to overcome is to derive a renewable ink for high-precision printing methods such as digital light processing (DLP) and liquid crystal display (LCD) [12,13]. These light-based printing methods require a photoresin, which is currently dominated by photoactive acrylates [14]. They are usually derived from non-renewable, petroleum sources [15]. Moreover, the resulting materials are crosslinked thermosets, which are hard to recycle [16]. The explosive growth of light-based 3D printing has led to massive disposal of the printed materials, thus creating serious, negative environmental impacts [17,18]. Although there are some recycling methods for thermosets based on physical recombination [19] or chemical depolymerization [20–23], either the reprocessed plastic shows degraded performance—resulting in downcycling—or they require high energy input and capital investment. Recently, dynamic chemical bonds (DCBs), such as dynamic imine bonds [24,25], boronic ester bonds [26,27], urethane [28,29], and silyl ether bonds [30], have been exploited to form dynamically crosslinked networks in the thermosets to achieve self-healing [24], remodeling [31], and welding [32]. Among these, dynamic transesterification reactions (DTER) have gained particular interest due to ease of implementation. DTER involves the exchange of ester groups and OR groups between different polymer chains, allowing for network rearrangement without permanent degradation of the material. Zhao et al. utilized DTER to enable the formation of DCBs between ester and hydroxyl groups, allowing for the reprocessability and reshaping of the structures [33]. Li et al. designed monomers that have ester and hydroxyl groups. These groups participate in DTER during the

heat treatment, leading to bond exchange reactions that allow for the upcycling of materials [34]. From the limited reports about thermoset recycling [35,36], we can catch a glimpse of their advantages over the traditional methods in terms of simple recycling procedures, low cost and energy input while maintaining impressive materials performance. Therefore, they are gaining interest from researchers in the 3D printing fields [37,38]. Despite the progress, the precursors used in those works are from petroleum sources. Moreover, no demonstration of the resulting materials has been made in fabricating tunable, healable, and recyclable mechanical metamaterials.

In this work, we demonstrate a new type of photoresin that is derived from epoxidized soybean oil (ESO), a renewable biomass precursor that is abundant for 3D printing of sustainable plastics because of their wide availability and low cost [39]. The reason why there is a lack of such a photoresin for DLP or LCD is that ESO as well as other biomass precursors have no or low intrinsic photoactivity. For example, the structures of ESO are mainly composed of triglyceride, while the photoactive unsaturated double bonds are located inside the fatty acid chains, thus showing little-to-no photoactivity. The photo-polymerization is difficult to trigger, preventing it from being directly used as a photoresin. Further, there are very few reports on introducing DCBs into renewable thermosets to tune their mechanical (tensile strength,  $\sigma_T$ , and fractural strain,  $\epsilon_T$ ), thermomechanical (phase transition temperature,  $T_g$ ), healing, and recycling properties when applied to 3D printing of the metamaterials.

To realize the goal of introducing DCBs into renewable thermosets, as shown in Fig. 1a-i, in this work, the triglyceride in the ESO was first converted to monoglyceride with grafted double bonds to obtain a highly photoactive monomer named epoxidized soybean oil-ethyl acrylamide (ESO-EA) by a transesterification reaction of ESO with HEAA (*N*-hydroxyethyl acrylamide). The monomer was then mixed with 2-hydroxy-3-phenoxypropyl acrylate (HA) and citric acid (CA) with varied weight ratios to form a photoresin for LCD printing. Here, HA is kept below 40 wt% to demonstrate renewability of the printed materials.

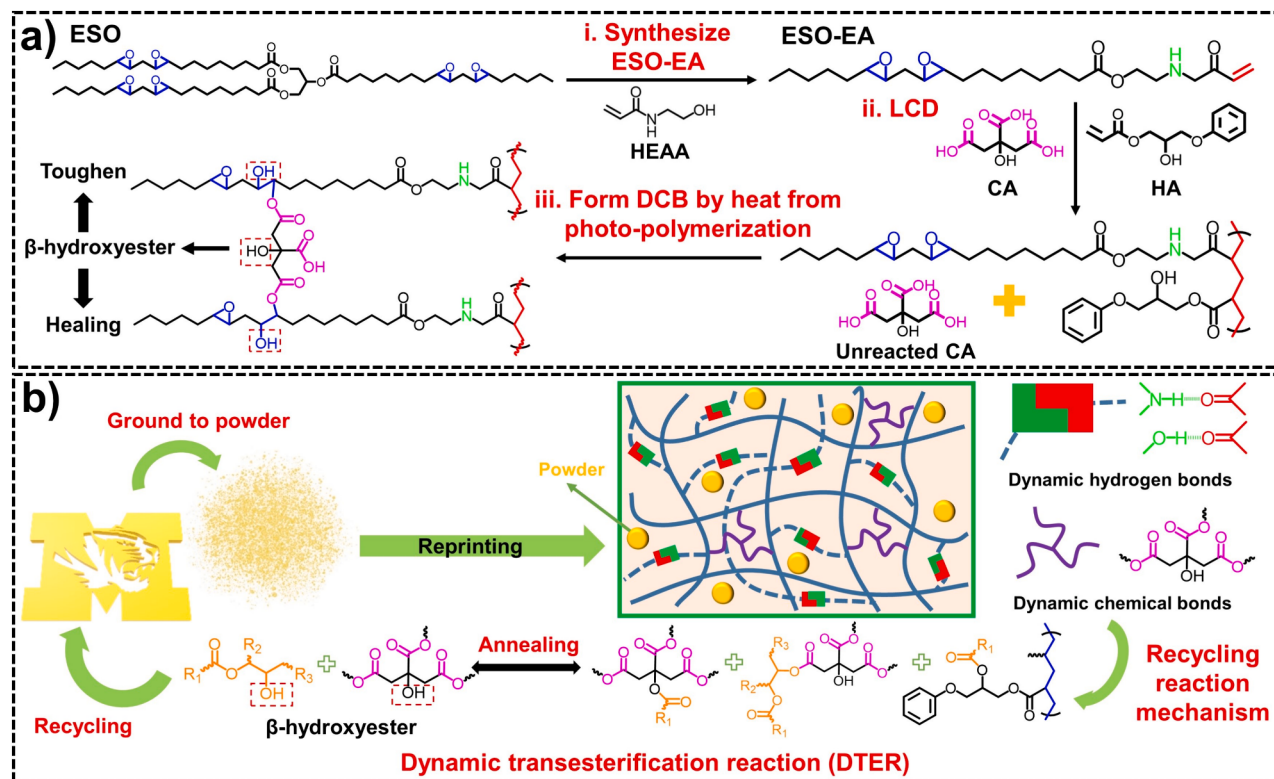


**Fig. 1.** (a) Schematic showing the synthesis of ESO-EA, photocuring reaction mechanism, and formation of LCCDN under UV. (b) Schematic showing the DTER mechanism for recycling.

Under UV irradiation, ESO-EA and HA were photopolymerized to linear ESO-EA/HA chains. Meanwhile, the heat generated by the photopolymerization initiates epoxy-acid reaction (EAR) between the epoxy group in the ESO-EA/HA chains and the carboxyl group in the CA (Fig. 1a-ii). These chemical bonds are dynamic—called dynamic chemical bonds (DCBs)—due to existence of the  $\beta$ -hydroxyester groups in the CA and ESO-EA/HA. These DCBs contribute to formation of low-density dynamic crosslinking network (LDDCN) (Fig. 1a-iii). This weak crosslinking reaction promotes solid–liquid separation to improve the printability and the mechanical strength while maintaining high stretchability of the resulting material. By thermal annealing, the  $\beta$ -hydroxyester and ester groups in the LDDCN can go through dynamic transesterification reaction (DTER) to increase the DCB density which modulates the materials properties ( $\sigma_T$ ,  $\varepsilon_T$ , and  $T_g$ ). Additionally, due to the DTER, the printed objects can be healed and recycled. The mechanism is schematically shown in Fig. 1b. During the transesterification reaction, the  $\beta$ -hydroxyester and ester groups from the polymer chain are exchanged and form new DCBs. It is worth noting that the  $\beta$ -hydroxyester groups act as a catalyst to promote the transesterification reaction. With this new renewable polymer with combinational properties, we demonstrate here property-tunability, healability, and recyclability in the LCD printed mechanical metamaterials.

## 2. Result and discussion

### 2.1. Synthesis of resin and study on properties of printed polymers

There are different types of DCBs like dynamic imine bonds, boronic ester bonds, urethane, and silyl ether bonds. These bonds are usually difficult to be constructed in photoactive monomers synthesized from biomass. Nevertheless, abundance of the ester groups in bio-resources

opens up new avenues for exploration. For instance, vegetable oil, one of the richest biomass components, would facilitate the DTER between the hydroxyl and ester groups possible [40]. Therefore, developing a vegetable oil-based photoresin with high photoactivity and DTER activity for LCD is desired. On the other hand, the internal double bonds of most vegetable oils can be oxidized to obtain epoxy vegetable oils, which is a mature process in industry. This provides another condition to react with carboxylic acid for forming DCBs and new  $\beta$ -hydroxyester groups via the EAR, thereby enabling high activity of DTER.

To make a photoactive resin, ESO was directly transesterified with HEAA to obtain ESO-EA, a monomer with epoxy groups and carbon–carbon double bonds, which not only has high photoactivity, but also provides conditions for DTFR. This results because the  $\beta$ -hydroxyester groups formed in the EAR step can be an effective green catalyst to promote the activity of DTER [34]. Based on this ink design, the resulting polymer is a low-density dynamic crosslinked network (LDDCN) supplemented by hydrogen bonding (Fig. 2a). All the resins with various carboxyl/epoxy ratios in the ESO-EA, HA, and CA show a viscosity of  $<1.3$  Pa·s at room temperature, which is suitable for the LCD printing (Fig. S1). The printed objects show fine features enabled by the high photoactivity of the resin and dual curing mechanism (Fig. 2b). One is the polymerization of ESO-EA and HA initiated by UV, while the other one is the EAR initiated by heat from polymerization. In addition, the printed objects show a shape memory property due to the LDDCN (Fig. 2c). The mechanism will be explained later. Its printed shape can be reprogrammed above the glass transition temperature ( $T_g$ ) and fixed below  $T_g$ . When heating it above  $T_g$ , the reprogrammed shape can recover to its originally printed shape. The demonstrated 3D printing of the developed shape memory polymers can also be named 4D printing [41].

The structure of ESO-EA was substantiated by the FTIR (Fig. 3a) and

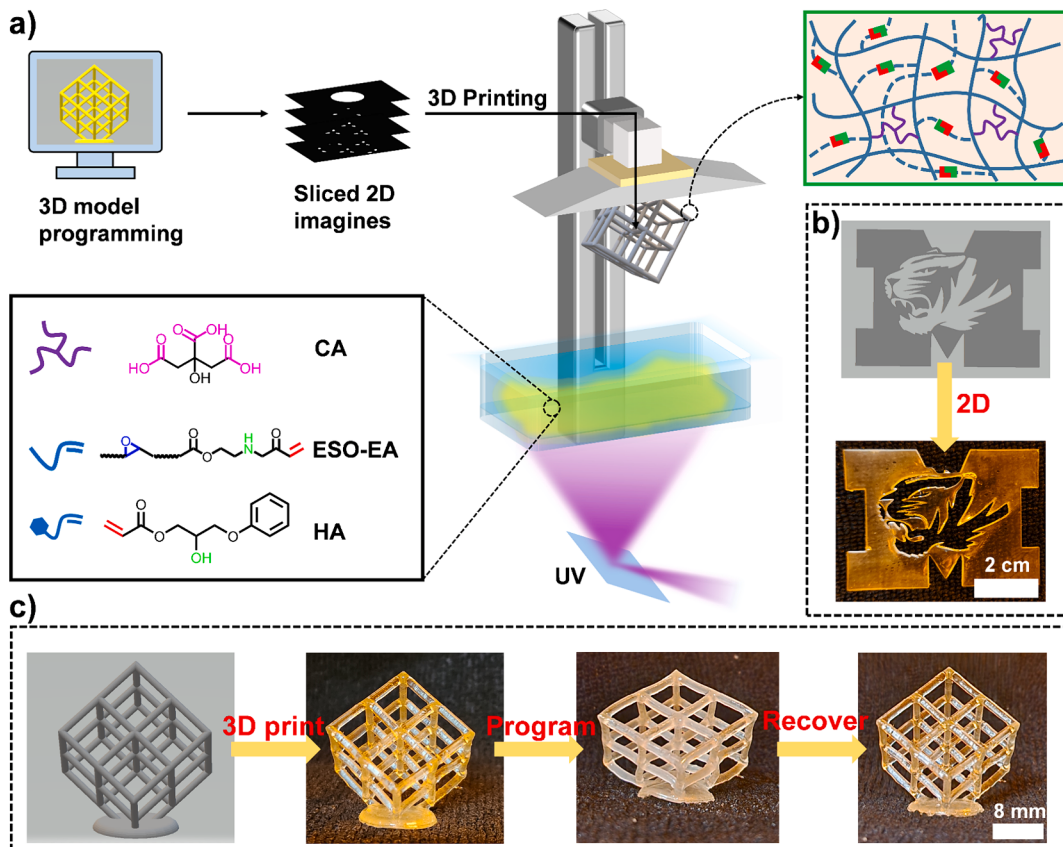


**Fig. 2.** (a) Schematic showing the ink formula, LCD printing, and resulting polymer network. (b) A photograph of a printed Mizzou logo. (c) Photographs showing a shape memory cycle of a printed 3D lattice made of a polymer with  $T_g$  of 36 °C.

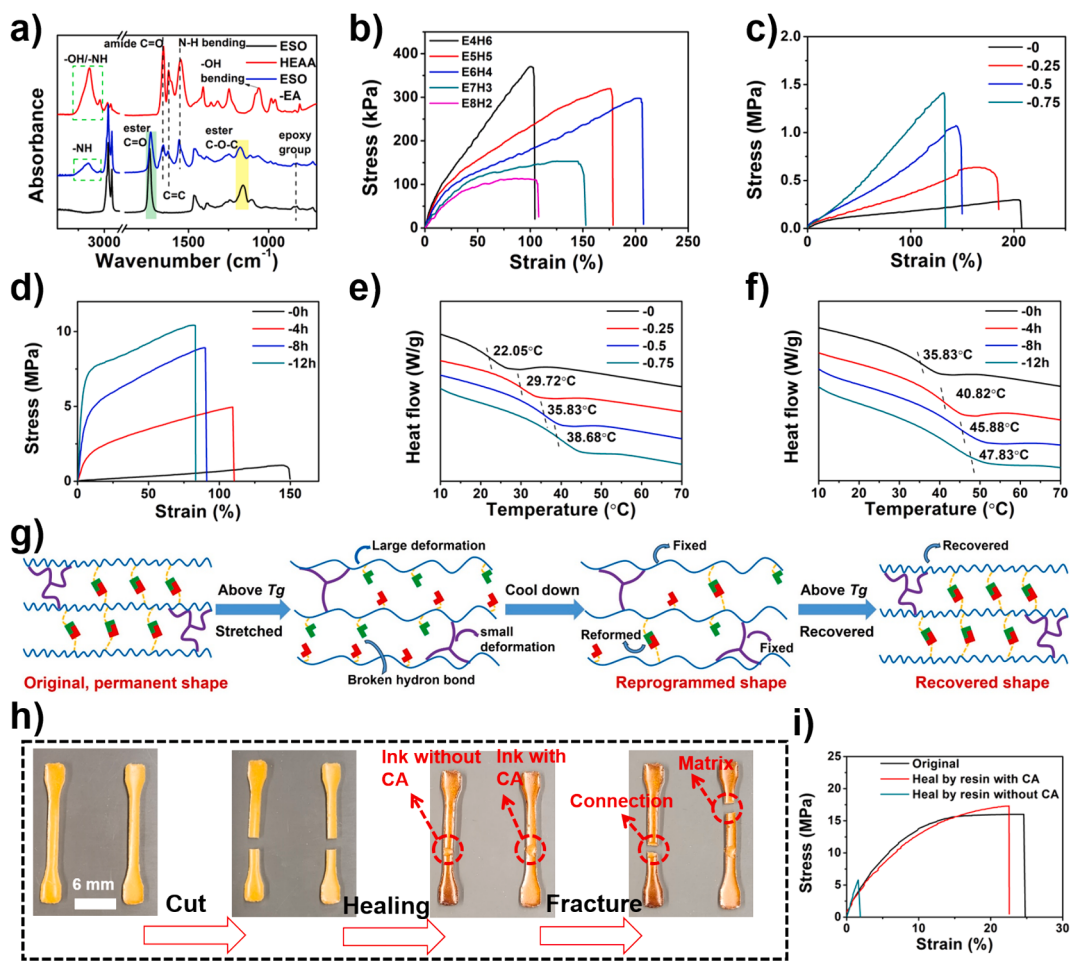


**Fig. 3.** (a) FTIR spectra of ESO, HEAA, and ESO-EA. (b) Stress–strain curves of ESO-EA/HA polymers with various ratio of HA and ESO-EA. (c) Stress–strain curves of ESO-EA/HA/CA polymers with varied carboxyl/epoxy molar ratios in the precursors. (d) Stress–strain curves of ESO-EA/HA/CA polymers after various-duration annealing.  $T_g$  of the ESO-EA/HA/CA polymers with varied carboxyl/epoxy molar ratios (e); annealed at 120 °C for varied durations (f). (g) Schematic explaining shape memory properties. (h) Photographs showing self-healing of polymers printed from the E6H4 resin with a carboxyl/epoxy ratio of 0.5. (i) Stress–strain curves of the polymers after self-healed with or without CA inks.

NMR (Fig. S2). Fig. 3a shows peaks at 1741 cm<sup>-1</sup> and 1161 cm<sup>-1</sup> corresponding to the stretching vibration modes of the ester C=O and C—O—C groups in the ESO. After the transesterification reaction, they shift to 1736 cm<sup>-1</sup> and to 1178 cm<sup>-1</sup> in ESO-EA, respectively. Meanwhile, the bending vibrational modes of the —OH groups from HEAA, peaked at 1059 cm<sup>-1</sup>, disappeared, while the bending vibration of the N-H peaked at 1558 cm<sup>-1</sup> and the stretching vibration of the amide C=O peaked at 1657 cm<sup>-1</sup> remain in the spectrum of the ESO-EA. The C=C bonds (stretching vibration peaked at 1628 cm<sup>-1</sup>) and the epoxy group (asymmetric stretching vibration peaked at 827 cm<sup>-1</sup>) are evident in the ESO-EA spectrum (Fig. 3a). The C=C bond empowers the photoactivity to the ESO-EA while the epoxy groups promote DTFR. As shown in Fig. S2, both the <sup>1</sup>H NMR and <sup>13</sup>C NMR spectra exhibit a clear structure of the ESO-EA, which agrees well with the FTIR results, confirming the successful synthesis of the ESO-EA monomer.

To optimize the ratio of ESO-EA and HA, the resins with different ratios were prepared for printing. The mechanical properties of the resulting polymers were compared (Fig. 3b). As the weight ratio of ESO-EA increases from 40 wt% to 60 wt%,  $\sigma_T$  slightly decreases from 370 to 298 kPa while  $\epsilon_T$  is greatly improved from 102 % to 205 %. Further increasing the ESO-EA content to 80 wt% reduces  $\sigma_T$  and  $\epsilon_T$  to 104 kPa and 110 %, respectively. This is because photopolymerization of ESO-EA and HA forms a linear polymer, where ESO-EA and HA work as soft and hard segments in the polymer network, respectively. The long chain structure of ESO-EA can effectively improve the stretchability of the

polymer, but it exhibits weakened strength. An excess of ESO-EA in the resin will cause the polymerized chains to be elastic but relatively weak. We found the optimum ratio between ESO-EA and HA is 6:4, termed as E6H4, after balancing the  $\sigma_T$  and  $\epsilon_T$  of the printed material for later materials processing. Thus, this ratio was chosen to study the effect of CA on the mechanical properties of the resulting materials as follows. Fig. 3c shows that introduction of CA greatly improves  $\sigma_T$  of the material. The one without CA has the lowest  $\sigma_T$  and the highest  $\epsilon_T$ .  $\sigma_T$  of the ones with CA are significantly improved by 121 % to 386 % depending on the mole ratio of the carboxyl groups in the CA and the epoxy groups in the ESO-EA, while their  $\epsilon_T$  are maintained at >130 %. That is because the heat generated by the photopolymerization can initiate EAR between the epoxy group in the ESO-EA/HA chains and the carboxyl group in the CA to form DCBs. If this hypothesis is valid, thermal annealing can increase the DCB density. The exothermic peak of the EAR from the DSC curve was identified to determine the optimal annealing temperature (Fig. S3). Generally, the curing temperature is when the reaction is the most violent. Here, we chose 120 °C, which is slightly higher than the curing temperature, as the optimal annealing temperature. Fig. 3d shows the effect of annealing durations at 120 °C for the samples with 0.5 mol ratio of the carboxyl groups in CA and the epoxy groups in ESO-EA. As the annealing time increases to 12 h,  $\sigma_T$  is improved to >10 MPa with  $\epsilon_T$  maintained at >80 % and toughness at ~7.7 MJ/m<sup>3</sup> (Fig. S4). The improved  $\sigma_T$  with high  $\epsilon_T$  can be attributed to the lowly crosslinked ESO-EA/HA network by DCBs and the hydrogen bond [42].

$T_g$ , a critical parameter determining the shape memory property as shown in Fig. 2c, was measured by DSC. Without CA, the ESO-EA/HA polymer printed from the E6H4 resin is a thermoplastic. Its  $T_g$  is 22.05 °C. With CA, the resulting one with 0.25 mol ratio of the carboxyl groups in CA and the epoxy groups in the E6H4 resin shows  $T_g$  of 29.72 °C. As the molar ratio of the carboxyl and epoxy groups increases to 0.75,  $T_g$  increases to 38.68 °C (Fig. 3e). Thermal annealing can further increase the DCB density, which make  $T_g$  increase to 47.83 °C (Fig. 3f). The wide tunability in  $T_g$  provides a potential for use in active metamaterials. The hypothesized mechanism is illustrated in the Fig. 3g. When the polymer is stretched above the  $T_g$ , the reversible ESO-EA/HA chains become soft and can therefore bear large deformations. This process is accompanied by breaking of the hydrogen bonds while the DCBs will be less affected. Lowering the temperature below  $T_g$  freezes the soft molecular chains. The frozen molecular chains together with the reformed hydrogen bonds will make the polymer remain stretched to fix the reprogrammed shape. Raising the temperature above  $T_g$  will reactivate the molecular chains, which are then relaxed with the favorable gain of entropy. This drives the reprogrammed temporary shape to recover to the original, permanent shape [43].

## 2.2. Study on tunable, healable properties of 3D printed mechanical metamaterials

The introduced DCBs give the ESO-EA/HA polymer the ability to break and form covalent bonds at different points of the network making self-healing and even the recycling of the polymer by these thermally activated reactions possible [44]. As the crystalline structures might restrict the chain mobility, which can result in inefficient healing, characterization of the crystallinity becomes important. To do that, we performed X-ray diffraction (XRD) on the processed polymer. As shown in Fig. S5, the polymer only displays a broad diffraction peak centered at 20 of 20°, indicating an amorphous structure at room temperature [45]. The thermal gravimetric analysis (TGA) data shows a decomposition temperature of ~200 °C, suggesting good thermal stability (Fig. S6a). The derivative thermogravimetry (DTG) data shows three main depolymerization processes: degradation of the ester groups at 200–350 °C, depolymerization of the C-C bonds at ~400 °C, and carbonization of the polymer at ~500 °C (Fig. S6b). Thus, annealing the material at 180 °C for healing is durable. This self-healing ability comes from DCBs. We hypothesize that the polymer network may form microscale phase separation from the hard CA formed DCBs and the soft ESO-EA/HA polymer chains. To validate it, we performed atomic force microscopy (AFM) imaging on the sample surface. The AFM image illustrates clear boundaries between soft (dark zones) and hard (bright zones) domains (Fig. S7), suggesting the phase separation [45]. The self-healing rate was then characterized by a stress relaxation test. The relaxation time, which is defined as the time required for  $G/G_0 = 1/e$ , reflects the rate of the polymer chain rearrangement. At 150 °C, the stress-relaxation is relatively slow, while the relaxation rate increases with increased temperature. When the temperature rises to 180 °C, the polymer chains quickly rearrange in <15 min (Fig. S8). This indicates that DTER strongly depends on the temperature, and the functional groups involved in DTER are more active at higher temperatures. To study the healing capability, the fractured samples were connected by resins with and without CA at the fracture points and then annealed in an oven at 180 °C (Fig. 3h). The results show that the sample healed by the resin with CA refractures at different locations from the original fracture point. That results because the DTER between the interfaces of the two fractured parts repairs the broken DCBs, thus largely restoring the mechanical performance of the original after repairing. This makes the healed location show comparable or even stronger mechanical strength compared to the non-fractured ones. Thus, the new fracturing point can be random. On the contrary, the sample healed by the resin without CA fractures at the same fracture point. Because the structure in this location is not healed via DTER and still the weakest point in the whole sample. To quantify

the mechanical properties of the healed samples, tensile testing was performed. As shown in Fig. 3i,  $\sigma_T$  and  $\varepsilon_T$  of the sample healed by the resin with CA are well maintained, while  $\sigma_T$  and  $\varepsilon_T$  of the one without CA are significantly reduced by 76 % and 92 %, respectively.

With the combinational study on the material properties, mechanical active metamaterials with tunable and healable properties were printed. As shown in Fig. 4a, a represented 3D origami structure which is expected to exhibit a gradual and distinctive bi-stable transformation due to the combined effects of compression deformation in the folded surfaces and twisting deformation along the folds was printed by LCD from the proposed polymer [46]. As expected, the origami shows a bi-stable mechanical response during a compression test as the compression deformation in the folded surfaces will be gradually transferred into a twisting deformation along the folding direction (Fig. 4b). The experimental curve is in good agreement with finite element analysis (FEA). By purposely creating two small cracks close to the base, the bi-stable deformation behavior empowered by the origami design disappears, as suggested by the well-agreed experimental and simulation compression force-displacement curves. Moreover, the fracture strain is decreased by ~40 % with the introduced cracks, while the tensile strength increases because the defect in the unit cell would make the structure stiffer. Both results indicate the sensitivity of the metamaterials to the damage of their constituting structural units, which validates the proposed hypothesis (Fig. 4c). After these cracks are self-healed, the bi-stable response curves are recovered with enhanced fractural strain (Fig. 4d), indicating the robustness of the metamaterials fabricated with our healable polymer.

In addition to studying the self-healing behavior, we evaluated the tunability of the shape memory properties. Unlike ordinary plastics that cannot recover their shape after a large deformation, the shape reprogramming capability of the developed polymer will allow the largely deformed origami to recover its original, permanent shape. Both simulated and experimental results underscore this shape recovery behavior (Fig. 4e). Shape memory also brings property adaptivity to this origami structure as the polymer can be switched back and forth between the glassy and rubbery states. As shown in Fig. 4f, when the structure is compressed by 76 % at room temperature (below  $T_g$ ), a bi-stable response curve appears, agreeing well with the one shown in Fig. 4b. When the temperature increases above the  $T_g$  at this compression strain there is a phase transition, and the material changes from a glassy to a rubbery state leading to a reduced Young's modulus, thus improving elasticity of the material. Immediately after this point, when the temperature is decreased below  $T_g$ , the material switches back to the glassy state, leading to the increased Young's modulus, thereby showing a tri-stable mechanical behavior with improved  $\sigma_T$  and  $\varepsilon_T$ , as shown in both the experimental and simulated curves (Fig. 4f). Here, we show that by controlling the temperature, this origami metastructure has tunability between bi-stable and tri-stable mechanical behaviors, demonstrating the uniqueness of using the shape memory materials in metamaterials fabrication. Combining the self-healing capabilities, to our best knowledge, this is the first demonstration of a tunable and healable metamaterial.

We hypothesize that the self-healing of the developed polymer can be used to not only repair the metamaterials, but also to heal multiple small units to a larger one to overcome the issue of the volume/size limit imposed by current light-based 3D printing. To validate this hypothesis, four origami structures were printed and assembled to a stacked larger structure (Fig. 4g). Then this 3D structure was put in oven for a healing process. When the compression test was performed, multi-stable mechanical responses were observed because of the repeated switch between bending deformation in the folded surfaces and twisting deformation along the folding direction (Fig. 4h). This indicates that the healed 3D structure is a new mechanical metamaterial consisting of four small constituent origami units. These multiple-state regions of force rising, falling and exceeding a certain threshold were coded into Signals 1, 2 and 3. When a force sensor was applied to the compressed 3D

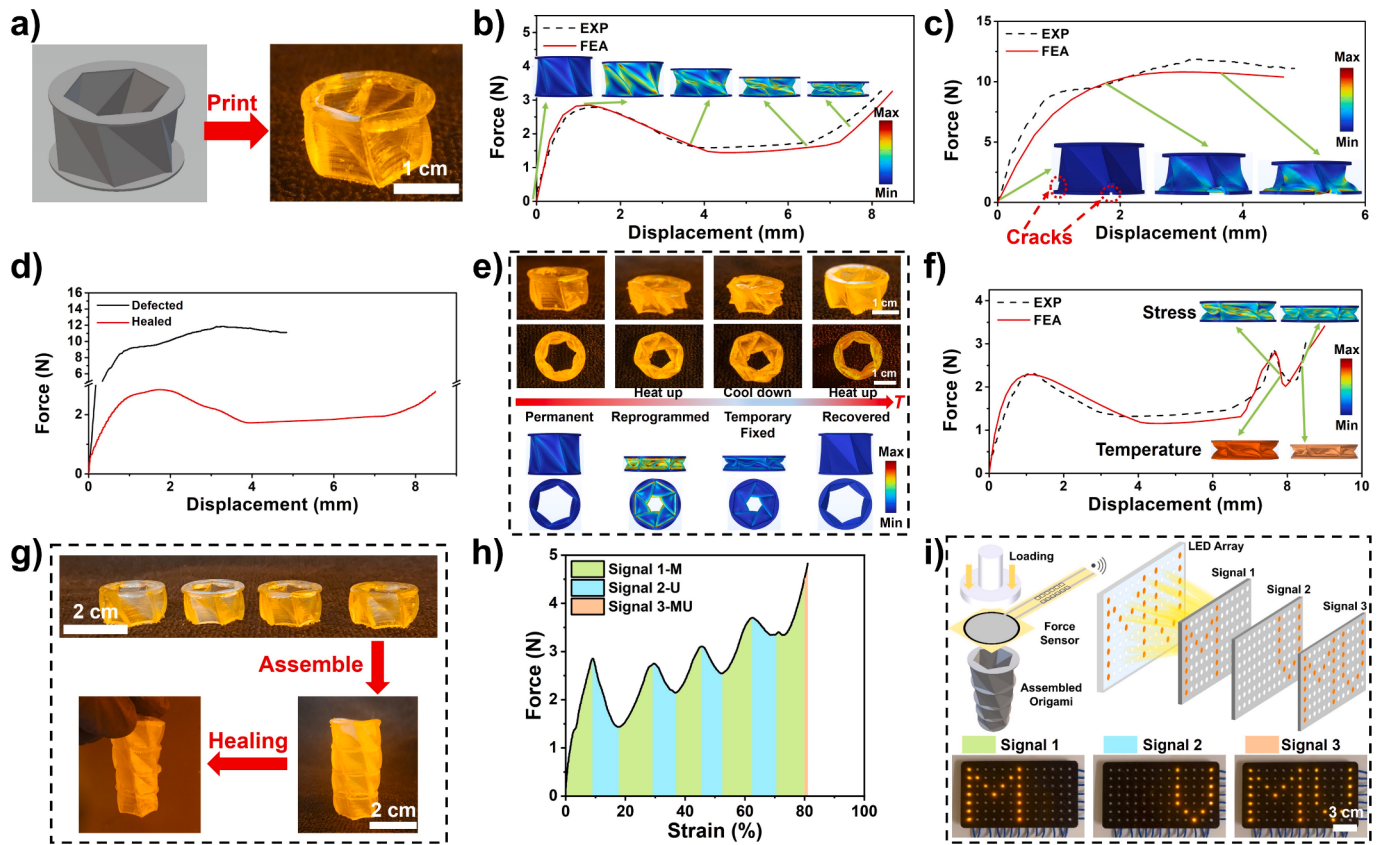


**Fig. 4.** (a) A designed and printed origami structure. (b) Experimental and FEA simulation force–displacement curves showing bi-stable mechanical response of an origami. (c) Experimental and FEA simulation force–displacement curves of an origami with small cracks in the base. (d) Experimental force–displacement curves of an origami with cracks and after the cracks were healed. (e) Photographs and FEA simulation results during the shape memory cycle of an origami structure. (f) Experimental and FEA simulation curves showing a tri-stable mechanical response of the printed origami. The third-stable state is endowed by the shape memory property. (g) Photographs showing assembly and healing of four small origami structures into a bigger one. (h) An experimental force–displacement curve showing a multi-stable mechanical response of the healed bigger origami. (i) Scheme and test of the programmed multi-stable response according to the sensed force and then is displayed by a LED array.

structure, these three regions can be sensed and then displayed by a light emitting diode (LED) array (Fig. S9), which can be programmed to “M”, “U” and “MU”, respectively, according to the sensed forces applied to the structure (Fig. 4i, Video S1).

### 2.3. Recyclability

The printed polymer is mainly composed of soybean oil and is therefore rich in the ester groups, which can be hydrolyzed under an alkaline solution. As shown in Fig. S10-S11, after immersion in alkaline aqueous solution for 150 min, the structure was completely degraded. Our previous work [47] suggests that it is possible that this degradation product can be recycled and reused, while the process would consume much time and energy. Direct recycling via DCBs could be a more efficient way. We evaluated the polymer recyclability via 3D printing. To do that, first, we ground the waste polymer into powder and added it as a filler to the photoresin for LCD printing [34]. Generally, the powder added to the resin increases the viscosity above the limiting viscosity, resulting in poor printability and lowered printing accuracy. To mitigate this issue, we experimentally found a maximum powder content of 20 wt % to ensure suitable viscosity (from 0.56 to 1.47 Pa·s) (Fig. S12) and good printing quality (Fig. S13). After that, the metamaterials were reprinted and then annealed at 180 °C to induce DTER so that the microstructure of the polymer network in the reprinted object was healed to form a complete part. The material can be recycled via the same process for at least three times (Fig. 5a). After three times of recycling, the printed structure still retains the shape memory function

(Fig. 5b). The tensile testing results show that  $\sigma_T$  of the first recycled material is improved by 2 % compared to the original one (Fig. 5c). This may be due to the increased DCB density caused by DTER. Even after recycling three times,  $\sigma_T$  is maintained at 93 %. To show that the DCBs on the surface of the ESO-EA/HA/CA polymer powder can be fully reformed via DTER without using the resin, the dry powder was loaded into a mold and then pressed into a new shape of polymer at 180 °C. The reshaped polymer shows  $\sigma_T$  of 17.96 MPa and  $\varepsilon_T$  of 21 %, which are 112 % and 85 % of the original  $\sigma_T$  and  $\varepsilon_T$ , respectively (Fig. 5d). This improvement in tensile strength may be due to the increased DCB density caused by DTER during the hot-pressing process. This forming method shows that the disclosed material can be well recycled even though it renders shapes with a constraint in the shape complexity.

### 3. Conclusion

The pursuit of mechanical metamaterials with tunable, healable, and recyclable properties has emerged as a grand challenge. To address this challenge, we used a renewable resource to formulate, a sustainable photoresin, for light-based 3D printing. By transforming ESO into a highly photoactive monomer (ESO-EA) and leveraging DCBs by including CA in the resin, a LDDCN was established within the printed polymer. This network, marked by its adaptability to external stimuli and enhanced mechanical attributes, was further empowered by DTER to render both self-healing and recyclability capabilities in the printed metamaterials. This work not only showcases the feasibility of creating property-tunable, healable, and recyclable metamaterials, but also

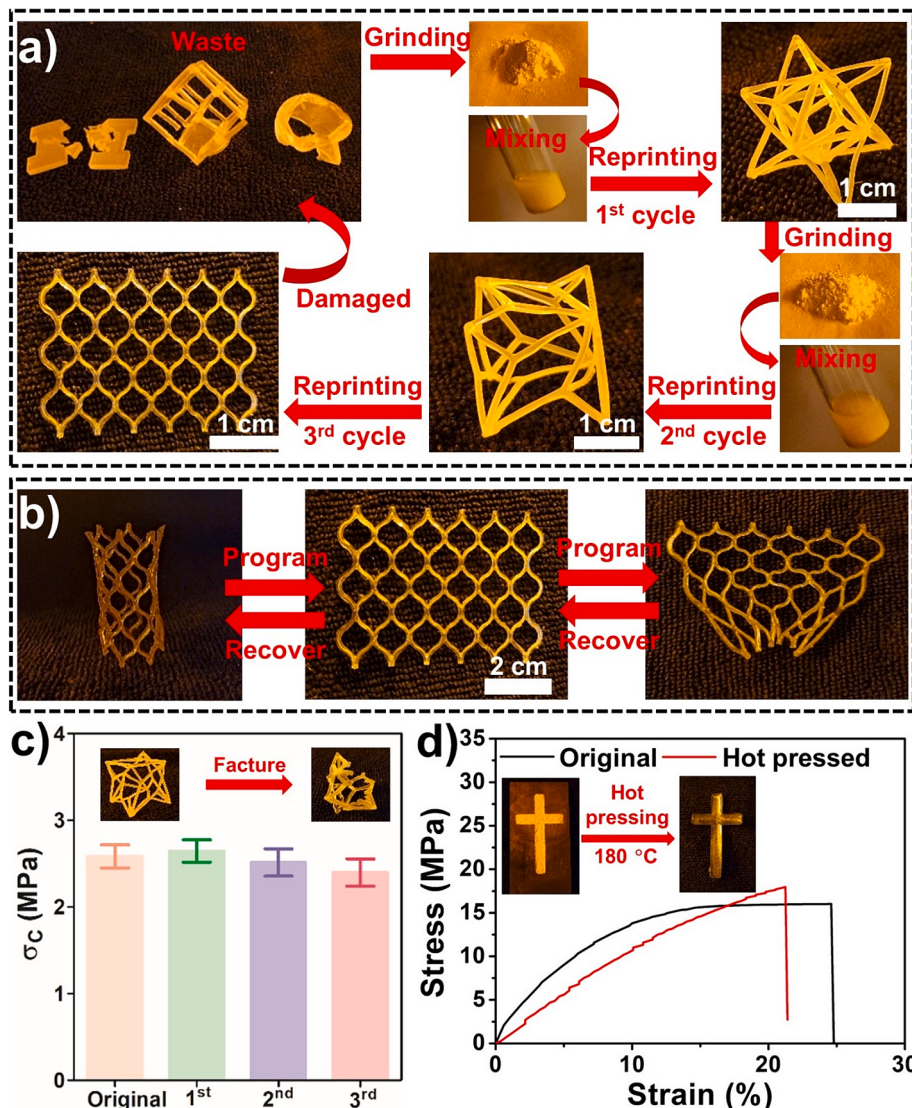


**Fig. 5.** (a) Photographs showing LCD based recycling of metamaterials via DTER. (b) Photographs showing shape memory performance of the third reprinted metamaterials. (c) Compression stresses of the reprinted metamaterials after different recycling times. (d) Stress–strain curves of an originally printed part and a fully recycled part from polymer powder by hot pressing at 180 °C. Inset images show the loaded powder in a mold and the reshaped part.

underscores the potential of utilizing renewable biomasses in new materials development. Integration of these advancements in LCD printed mechanical metamaterials heralds a promising era of sustainable and adaptable material design, making metamaterial fabrication greener and more versatile.

#### 4. Methods

##### 4.1. Materials

Epoxidized Soybean Oil (ESO, average epoxy groups of 4.1 per tri-glyceride) was purchased from Aladdin Industrial (Shanghai, China). 2-Hydroxy-3-phenoxypropyl acrylate (HA), citric acid monohydrate (CA, > 99 %), sodium chloride (NaCl, > 99 %), sodium hydroxide (NaOH, > 97 %), Tetrahydrofuran (THF, > 99.9 %), Zinc acetylacetone (Zn(acac)<sub>2</sub>) and *N*-hydroxyethyl acrylamide (HEAA, > 97 %) were purchased from Sigma Aldrich (St. Louis, MO, U.S.). Diphenyl(2,4,6-trimethylbenzoyl)phosphine oxide (TPO, >97 %) was purchased from Fisher Scientific (Pittsburgh, PA, U.S.). These materials were used without further purification.

##### 4.2. Synthesis of ESO-EA

ESO (0.15 mol) was charged into a 500 mL flask and dissolved by THF (150 mL). Then, HEAA (1 mol) were added in the solution. The reaction was performed at 40 °C under atmospheric condition in the presence of NaOH (5 g) as catalysts and stopped when the solution was completely homogenized. The obtained product was purified with saturated NaCl solution, and then dried under vacuum to obtain ESO-EA monomer with epoxy functional groups and carbon–carbon double bonds at a yield of 91.6 %.

##### 4.3. Resin preparation and printing

ESO-EA and HA were mixed at weight ratios of 4:6, 5:5, 6:4, 7:3, and 8:2, named E4H6, E5H5, E6H4, E7H3, and E8H2, to study effect of the two monomers on the studied properties. The optimized E6H4 was used for other studies. To do that, CA with the amount calculated based on the carboxylic acid equivalents/epoxy equivalents of 0.25, 0.5, and 0.75 was added into the E6H4 resin. After objects were printed, they were post-cured by 405-nm UV light for 60 s and annealed in an oven at 120 °C for 4, 8, and 12 h. All the resins were added with 2 wt% TPO as

photoinitiator, and 5 mol% of Zn(acac)<sub>2</sub> as a catalyst (relative to the amount of the –COOH groups). The printing was done on a liquid crystal display (LCD) printer (Anycubic Photon Mono X) with an irradiation wavelength of 405 nm under a power density of ~5 mW/cm<sup>2</sup>. The layer thickness was set to 50 μm and the exposure time was set to 15 s. Self-healing evaluation test was conducted on the sample annealed at 180 °C for 4 h.

#### 4.4. Reprinting and recycling

The polymer was recycled via 3D printing. The waste polymer was ground into powder. And then 20 wt% of powder was added as a filler into the photoresin for LCD printing. After that, the metamaterials were reprinted and then annealed at 180 °C to induce DTER so that the microstructure of the polymer network in the reprinted object was healed to form a complete part.

#### 4.5. FEA simulation

COMSOL Multiphysics was used to conduct simulation on several metamaterials' models under compression test. The stationary study was used in the Solid Mechanics Interface. The basic model was built in Solidworks and then imported to COMSOL for simulation. In the simulation, the hyperelastic Neo-Hookean model with Young's modulus 3.49 MPa and Poisson's ratio 0.3 is considered. The contact pair was added on the side wall to simulate the contact process when the model was under compression. To simulate the compression behavior of the origami structure, the top surface was applied by a vertically downward varying displacement with a uniform step 1 mm, whereas the bottom surface was fixed and the reaction force is calculated for each displacement.

To simulate the compression behavior of the origami with cracks on the model, three equidistant cracks were opened at the bottom of the model, where one side wall was intersected with the other side wall. These locations are most likely to affect the origami structure. It also facilitates data collection and saves simulation time. The same boundary conditions and contact pairs were set as the ones in the first set of simulations, while the step displacement step was set as 1 mm in the beginning stages and 0.5 mm when the reaction force rapidly increased.

To simulate the shape memory behavior of the origami [46], the model parameters for the force–displacement function were changed to displacement dependent functions in the physical properties of the material. The interval function is increased by 20 % to 40 % to simulate changes in the model's physical properties due to the aroused temperatures. Then this parameter was reduced by 10 %–20 % to simulate the physical properties of the material gradually returning to the initial state after the external temperature returns to the initial value. At the critical points where the force changes rapidly, the step displacement was set between 0.3 to 0.5 mm.

#### 4.6. Materials characterization

The chemical structure of the synthesized ESO-EA was characterized by attenuated total reflectance Fourier transform infrared (ATR-FTIR) and nuclear magnetic resonance (NMR) spectroscopies. ATR-FTIR spectra were collected by a Thermo Nicolet 380 FTIR spectrometer with DIAMOND ATR. NMR were collected by a Bruker Avance III UltraStabilized 800 MHz Spectrometer. A Rigaku SmartLab II with a zero background holder was used to collect XRD spectra. A scan width of 0.05° per step and a scan rate of 7°/min were used to scan the samples in the range of 10° to 90°. The viscosity of ink was evaluated by a modular rotation and interface rheometer equipped with a C60/2° (MCR302). The test was performed at room temperature with shear rates changing from 0.1 to 100 1/s. Stress-relaxation test was also conducted on the same rheometer at 150, 160, 170, and 180 °C. The samples were first equilibrated at the testing temperatures for 15 min. After that, a constant normal force was applied for good contact and an instantaneous 1 %

strain was applied on the sample. The resultant stress was monitored with respect to time. The glass transition temperature ( $T_g$ ) of the polymer was obtained from differential scanning calorimetry (DSC) by using a DSC Q20 machine (TA Instruments, Newcastle, DE, USA). Sample (~15 mg) was placed in a standard aluminum crucible with a lid and scanned in a dynamic mode from –10 to 100 °C at a heating rate of 10 °C/min under N<sub>2</sub> atmosphere (30 mL/min). The mechanical property was tested on a Mark-10 universal testing machine at a moving rate of 50 mm/min<sup>–1</sup>. The mechanical property tests were conducted according to ASTM D638 standard for tensile testing. The sample size was Type IV specimen as per ASTM D638. The Mark-10 universal testing machine was equipped with FS05-2/FS05-50 Force Sensor with a range of 0.5–250 N and an accuracy of ±0.1 % of full scale. For each composition, we tested a minimum of four specimens. A TA Instruments TGA/DSC 3+ was used for TGA data collection in an open-air environment. The heating rate of 10 °C/min was applied to elevate the temperature until 800 °C. Non-contact mode measurements for surface phases and amplitudes that arise from the surface characteristics was used. Atomic force microscopy (AFM) images are obtained from a Park System NX-20, NCHR-10 (silicon SPM-Sensor), thickness: 4 μm, length:125 μm, width:30 μm, detector side is coated with Al. Resonance frequency: 320 kHz, Force constant: 42 N/m.

#### Author contributions

Y.W. conceptualized and designed the project, and performed the experiments in monomer synthesis, ink preparation, printing, and recycling. He also collected and analyzed the data. K.J.S. contributed to XRD and TGA/DTG under supervision of J.M.T. J.S. collected AFM images under supervision of J.M.T. Q.C. performed the FEA simulation with suggestions from G.H. and S.W. B.Z. contributed to the experiment on the bulb array fabrication and testing. Z.C. contributed to 3D model design. J.L. organized the tasks, supervised the team, oversaw the progress of the project, and laid the architecture of manuscript. Y.W. wrote the first draft which was thoroughly revised by J.L. All authors read, corrected and commented the manuscript, and agreed to the final version.

#### CRediT authorship contribution statement

**Yuchao Wu:** Writing – original draft, Validation, Methodology, Conceptualization. **Cheng Qiu:** Validation, Methodology. **Karla J. Silva:** Validation, Methodology. **Jaeho Shin:** Validation. **Shaoyun Wang:** Writing – review & editing, Methodology. **Bujingda Zheng:** Validation, Methodology. **Zhenru Chen:** Methodology. **Guoliang Huang:** Writing – review & editing. **James M. Tour:** Writing – review & editing. **Jian Lin:** Writing – review & editing, Supervision, Conceptualization.

#### Declaration of competing interest

The authors declare that they have no known competing financial interests or personal relationships that could have appeared to influence the work reported in this paper.

#### Data availability

Data will be made available on request.

#### Acknowledgement

J. L. and J. M. T. thank U.S. Army Corps of Engineers, ERDC (grant number: W912HZ-21-2-0050) for the financial support.

## Appendix A. Supplementary data

Supplementary data to this article can be found online at <https://doi.org/10.1016/j.cej.2024.156138>.

## References

- [1] X. Zheng, H. Lee, T.H. Weisgraber, M. Shusteff, J. DeOtte, E.B. Duoss, J.D. Kuntz, M.M. Biener, Q. Ge, J.A. Jackson, Ultralight, ultrastiff mechanical metamaterials, *Science* 344 (2014) 1373–1377.
- [2] Y. Chen, X. Li, C. Scheibner, V. Vitelli, G. Huang, Realization of active metamaterials with odd micropolar elasticity, *Nat. Commun.* 12 (2021) 5935.
- [3] M. Bodaghi, W. Liao, 4d printed tunable mechanical metamaterials with shape memory operations, *Smart Mater. Struct.* 28 (2019) 045019.
- [4] G. Ji, J. Huber, Recent progress in acoustic metamaterials and active piezoelectric acoustic metamaterials-a review, *Appl. Mater. Today* 26 (2022) 101260.
- [5] S.M. Montgomery, S. Wu, X. Kuang, C.D. Armstrong, C. Zemelka, Q. Ze, R. Zhang, R. Zhao, H.J. Qi, Magneto-mechanical metamaterials with widely tunable mechanical properties and acoustic bandgaps, *Adv. Funct. Mater.* 31 (2021) 2005319.
- [6] M. Pishvar, R.L. Harne, Foundations for soft, smart matter by active mechanical metamaterials, *Adv. Sci.* 7 (2020) 2001384.
- [7] Q. Wu, X. Xu, H. Qian, S. Wang, R. Zhu, Z. Yan, H. Ma, Y. Chen, G. Huang, Active metamaterials for realizing odd mass density, *PNAS* 120 (2023) e2209829120.
- [8] Y. Chen, X. Li, G. Hu, M.R. Haberman, G. Huang, An active mechanical willis meta-layer with asymmetric polarizabilities, *Nat. Commun.* 11 (2020) 3681.
- [9] H. Deng, X. Xu, C. Zhang, J.-W. Su, G. Huang, J. Lin, Deterministic self-morphing of soft-stiff hybridized polymeric films for acoustic metamaterials, *ACS Appl. Mater. Interfaces* 12 (2020) 13378–13385.
- [10] Q. Wang, J.A. Jackson, Q. Ge, J.B. Hopkins, C.M. Spadaccini, N.X. Fang, Lightweight mechanical metamaterials with tunable negative thermal expansion, *Phys. Rev. Lett.* 117 (2016) 175901.
- [11] X. Zheng, W. Smith, J. Jackson, B. Moran, H. Cui, D. Chen, J. Ye, N. Fang, N. Rodriguez, T. Weisgraber, Multiscale metallic metamaterials, *Nat. Mater.* 15 (2016) 1100–1106.
- [12] D.A. Walker, J.L. Hedrick, C.A. Mirkin, Rapid, large-volume, thermally controlled 3d printing using a mobile liquid interface, *Science* 366 (2019) 360–364.
- [13] Y. Wu, Y. Zeng, Y. Chen, C. Li, R. Qiu, W. Liu, Photocurable 3d printing of high toughness and self-healing hydrogels for customized wearable flexible sensors, *Adv. Funct. Mater.* 31 (2021) 2107202.
- [14] S.C. Ligon, R. Liska, J. Stampfl, M. Gurr, R. Mülhaupt, Polymers for 3d printing and customized additive manufacturing, *Chem. Rev.* 117 (2017) 10212–10290.
- [15] B.C. Gross, J.L. Erkal, S.Y. Lockwood, C. Chen, D.M. Spence, Evaluation of 3d printing and its potential impact on biotechnology and the chemical sciences, *Anal. Chem.* 86 (2014) 3240–3253.
- [16] T. Kaiser, Highly crosslinked polymers, *Prog. Polym. Sci.* 14 (1989) 373–450.
- [17] H. Wu, W. Fahy, S. Kim, H. Kim, N. Zhao, L. Pilato, A. Kafi, S. Bateman, J. Koo, Recent developments in polymers/polymer nanocomposites for additive manufacturing, *Prog. Mater. Sci.* 111 (2020) 100638.
- [18] L.J. Tan, W. Zhu, K. Zhou, Recent progress on polymer materials for additive manufacturing, *Adv. Funct. Mater.* 30 (2020) 2003062.
- [19] C. Jehanno, J.W. Alty, M. Roosen, S. De Meester, A.P. Dove, E.Y.X. Chen, F. A. Leibfarth, H. Sardon, Critical advances and future opportunities in upcycling commodity polymers, *Nature* 603 (2022) 803–814.
- [20] J.-B. Zhu, E.M. Watson, J. Tang, E.-Y.-X. Chen, A synthetic polymer system with repeatable chemical recyclability, *Science* 360 (2018) 398–403.
- [21] P.R. Christensen, A.M. Scheuermann, K.E. Loeffler, B.A. Helms, Closed-loop recycling of plastics enabled by dynamic covalent diketoenamine bonds, *Nat. Chem.* 11 (2019) 442–448.
- [22] B.A. Abel, R.L. Snyder, G.W. Coates, Chemically recyclable thermoplastics from reversible-deactivation polymerization of cyclic acetals, *Science* 373 (2021) 783–789.
- [23] M. Häußler, M. Eck, D. Rothauer, S. Mecking, Closed-loop recycling of polyethylene-like materials, *Nature* 590 (2021) 423–427.
- [24] D. Montarnal, M. Capelot, F. Tournilhac, L. Leibler, Silica-like malleable materials from permanent organic networks, *Science* 334 (2011) 965–968.
- [25] P. Taynton, K. Yu, R.K. Shoemaker, Y. Jin, H.J. Qi, W. Zhang, Heat- or water-driven malleability in a highly recyclable covalent network polymer, *Adv. Mater.* 26 (2014) 3938–3942.
- [26] M. Röttger, T. Domenech, R. van der Weegen, A. Breuillac, R. Nicolaï, L. Leibler, High-performance vitrimers from commodity thermoplastics through dioxaborolane metathesis, *Science* 356 (2017) 62–65.
- [27] J.J. Cash, T. Kubo, A.P. Bapat, B.S. Sumerlin, Room-temperature self-healing polymers based on dynamic-covalent boronic esters, *Macromolecules* 48 (2015) 2098–2106.
- [28] W. Denissen, G. Rivero, R. Nicolaï, L. Leibler, J.M. Winne, F.E. Du Prez, Vinyllogous urethane vitrimers, *Adv. Funct. Mater.* 25 (2015) 2451–2457.
- [29] D.J. Fortman, J.P. Brutman, C.J. Cramer, M.A. Hillmyer, W.R. Dichtel, Mechanically activated, catalyst-free polyhydroxyurethane vitrimers, *J. Am. Chem. Soc.* 137 (2015) 14019–14022.
- [30] Y. Nishimura, J. Chung, H. Muradyan, Z. Guan, Silyl ether as a robust and thermally stable dynamic covalent motif for malleable polymer design, *J. Am. Chem. Soc.* 139 (2017) 14881–14884.
- [31] X. Chen, M.A. Dam, K. Ono, A. Mal, H. Shen, S.R. Nutt, K. Sheran, F. Wudl, A thermally re-mendable cross-linked polymeric material, *Science* 295 (2002) 1698–1702.
- [32] C. Li, Y. Chen, Y. Zeng, Y. Wu, W. Liu, R. Qiu, Strong and recyclable soybean oil-based epoxy adhesives based on dynamic borate, *Eur. Polym. J.* 162 (2022) 110923.
- [33] B. Zhang, K. Kowsari, A. Serjouei, M.L. Dunn, Q. Ge, Reprocessable thermosets for sustainable three-dimensional printing, *Nat. Commun.* 9 (2018) 1831.
- [34] H. Li, B. Zhang, R. Wang, X. Yang, X. He, H. Ye, J. Cheng, C. Yuan, Y.F. Zhang, Q. Ge, Solvent-free upcycling vitrimers through digital light processing-based 3d printing and bond exchange reaction, *Adv. Funct. Mater.* 32 (2022) 2111030.
- [35] C.J. Kloxin, C.N. Bowman, Covalent adaptable networks: Smart, reconfigurable and responsive network systems, *Chem. Soc. Rev.* 42 (2013) 7161–7173.
- [36] Y. Jin, C. Yu, R.J. Denman, W. Zhang, Recent advances in dynamic covalent chemistry, *Chem. Soc. Rev.* 42 (2013) 6634–6654.
- [37] Q. Shi, K. Yu, X. Kuang, X. Mu, C.K. Dunn, M.L. Dunn, T. Wang, H.J. Qi, Recyclable 3d printing of vitrimer epoxy, *Mater. Horiz.* 4 (2017) 598–607.
- [38] B. Zhang, K. Kowsari, A. Serjouei, M.L. Dunn, Q. Ge, Reprocessable thermosets for sustainable three-dimensional printing, *Nat. Commun.* 9 (2018) 1–7.
- [39] Y. Wu, M. Fei, T. Chen, R. Qiu, W. Liu, Fabrication of degradable and high glass-transition temperature thermosets from palm oil and isosorbide for fiber-reinforced composites, *Ind. Crops Products* 170 (2021) 113744.
- [40] M.A. Lucherelli, A. Duval, L. Avérous, Biobased vitrimers: Towards sustainable and adaptable performing polymer materials, *Prog. Polym. Sci.* (2022), 101515.
- [41] M. Falahati, P. Ahmadvand, S. Safaei, Y.-C. Chang, Z. Lyu, R. Chen, L. Li, Y. Lin, Smart polymers and nanocomposites for 3d and 4d printing, *Mater. Today* 40 (2020) 215–245.
- [42] B. Zhang, H. Li, J. Cheng, H. Ye, A.H. Sakhaei, C. Yuan, P. Rao, Y.-F. Zhang, Z. Chen, R. Wang, X. He, J. Liu, R. Xiao, S. Qu, Q. Ge, Mechanically robust and uv-curable shape-memory polymers for digital light processing based 4d printing, *Adv. Mater.* 33 (2021) 2101298.
- [43] S. Mu, Y. Zhang, J. Zhou, B. Wang, Z. Wang, Recyclable and mechanically robust palm oil-derived epoxy resins with reconfigurable shape-memory properties, *ACS Sustain. Chem. Eng.* 8 (2020) 5296–5304.
- [44] F.I. Altuna, V. Pettarin, R.J. Williams, Self-healable polymer networks based on the cross-linking of epoxidised soybean oil by an aqueous citric acid solution, *Green Chem.* 15 (2013) 3360–3366.
- [45] D. Wang, J. Xu, J. Chen, P. Hu, Y. Wang, W. Jiang, J. Fu, Transparent, mechanically strong, extremely tough, self-recoverable, healable supramolecular elastomers facilely fabricated via dynamic hard domains design for multifunctional applications, *Adv. Funct. Mater.* 30 (2020) 1907109.
- [46] R. Tao, L. Ji, Y. Li, Z. Wan, W. Hu, W. Wu, B. Liao, L. Ma, D. Fang, 4d printed origami metamaterials with tunable compression twist behavior and stress-strain curves, *Compos. Part B: Eng.* 201 (2020) 108344.
- [47] Y. Wu, P.A. Advincula, O. Giraldo-Londoño, Y. Yu, Y. Xie, Z. Chen, G. Huang, J. M. Tour, J. Lin, Sustainable 3d printing of recyclable biocomposite empowered by flash graphene, *ACS Nano* 16 (2022) 17326–17335.